Dynamics of High-velocity Domain Wall Motion and Spin Wave Excitation in Trilayer Structures

*Xingtai Chen,[1] Thomas J. Hayward,[2] Wenqing Liu,[1] Matthew T. Bryan,[1,] ***

[1] Department of Electronic Engineering, Royal Holloway, University of London, UK

[2] Department of Materials Science and Engineering, University of Sheffield, UK

*Authors to whom correspondence should be addressed. Email: Matthew.Bryan@rhul.ac.uk

Abstract Propagation of dipolar-coupled transverse domain walls in a Permalloy/Non-magnetic/Permalloy trilayer was investigated using micromagnetic modeling. Circulating stray fields meant that the walls adopted a composite structure with behavior analogous to walls seen in nanotubes. Wall velocities were sensitive to the chirality of the stray field circulation, with velocities of the most favored chirality enhanced by 32% compared with velocities seen in the individual constituent layers just below their Walker breakdown field. Additionally, Walker breakdown was completely suppressed within the trilayer for both chiralities, despite occurring in the constituent layers when modelled in isolation, leading to a maximum of 317% velocity enhancement. Wall velocity saturated around 1100 m/s due the Cherenkov-like emission of spin waves, comparable to the magnonic regime of nanotubes. By reproducing the advantageous domain wall dynamics of nanotubes within a planar system, we demonstrate that ultrafast magnetic switching may feasibly be realized within a lithographically produced system.

1. Introduction

Magnetic domain walls in ferromagnetic nanostructures play an essential role in several proposed applications, such as magnetic memories[1] magnetic logic,[2] and magnetic field sensors.[3] Due to the ease of fabrication using lithographic methods, many of these devices are constructed from planar wire geometries. Depending on the size and composition of the wires, a variety of different types of domain wall may be present,[4,5,6] which can influence device operation. Materials where shape anisotropy dominates, such as Permalloy ($Ni_{80}Fe_{20}$), support head-to-head (tail-to-tail) domain walls, in which the wall forms between in-plane domains pointing along the wire axis towards (away from) the domain wall. The simplest type of head-to-head wall is the transverse wall, a purely in-plane rotation of magnetization. As the wire width and thickness increases, the normally symmetric transverse wall first transitions into an asymmetric transverse structure and then into a vortex,[5] where the magnetization circulates around the center of the wall, followed by more complex wall structures at very large dimensions.[4,6]

Domain walls may be propagated along a wire using a magnetic field,[7,8] or alternatively applied currents,[9,10] spin waves[11,12] or stress gradients.[13,14] At low fields, walls maintain their structure and move with a velocity v that increases linearly with field H, consistent with one-dimensional approximations[15]

$$v = \frac{\gamma_0 \Delta}{\alpha} H \qquad (1)$$

where, γ_0 is the gyromagnetic γ ratio multiplied by the vacuum permeability μ_0, Δ is the domain wall width, α is the Gilbert damping constant. Above a threshold field (the Walker breakdown field), walls undergo a periodic transformation of the wall chirality (in transverse walls occurring via the nucleation of either a vortex or anti-vortex[16]), accompanied by a transient retrograde wall motion. [15,17] Due to the retrograde motion, the onset of Walker breakdown is associated with an abrupt decrease in the wall velocity.[18] At fields much higher than the Walker breakdown field, wall motion becomes chaotic, leading to a recovery of positive wall mobility and progressively faster wall motion.[16] Interactions between neighboring wires can significantly alter domain wall behavior. Stray field interactions between domain walls in adjacent wires can either result in pinning of a moving wall or depinning of a pinned wall.[19,20] Once depinned, pairs of walls may become coupled, enabling one wall to drive propagation and even induce Walker breakdown in the other purely through stray field interactions.[21] Coupling between domain walls in nanowires with perpendicular anisotropy has been shown to enhance wall velocity. Hrabec et al. demonstrated that dipolar-coupled Néel walls with opposing

magnetizations could be stabilized in a multilayer by control of the Dzyaloshinskii-Moriya interaction (DMI) and that the coupled walls travelled almost twice as fast as non-coupled walls in the same system.[22] Similar coupling of transverse domain walls has not yet been demonstrated.

Walker breakdown introduces uncertainty into switching, as depinning from structural features and defects exhibits stochasticity that strongly depends on the precise domain wall configuration.[23] Since pinning interactions are necessary for many proposed applications, much work has focused on suppressing the Walker breakdown process. Kunz and Reiff showed theoretically that Walker breakdown could be suppressed using strong (~1500 Oe) out-of-plane fields to reverse anti-vortex core magnetization and therefore control the core trajectory.[24] Alternatively, somewhat weaker (~250 Oe) transverse fields have been experimentally demonstrated to suppress Walker breakdown,[25] with modelling indicating that the transverse field facilitates the wall to separate from nucleated antivortices before retrograde motion can take place.[26] Another route to suppressing Walker breakdown is through the structural design of the wire. Burn et al. demonstrated that antivortex nucleation was suppressed in wires with a sinusoidal edge profile, if the edge amplitude varied significantly over length-scales shorter than the spatial separation of the wall transitions during Walker breakdown.[27] However, while edge modulations remove the need for an additional field component on top of the drive field, they are not an ideal solution to suppress Walker breakdown as they also introduce pinning sites that inhibit motion at low fields.

Moving from a planar to a 3D geometry could offer a way to circumvent the issue of edge pinning. Yan et al. reported that tubular nanowires support domain walls that circulate around the wire like a ring, analogous to a transverse wall in planar systems.[28] In addition to suppressing Walker breakdown by removing the edge boundary from which the antivortex nucleates, the curved geometry induces a radial magnetization component to the domain wall that produces a torque that inhibits Walker breakdown.[29,30] This suppresses Walker breakdown so completely that domain wall velocities can become fast enough to produce a Cherenkov-like effect for magnons.[28,31] While these properties provide the potential to develop novel applications that exploit them, the three-dimensional structure of a tube means that fabrication is not feasible with standard (planar) lithographic techniques. In this work, we used micromagnetic modeling to investigate whether magnetization texture within planar structures could be manipulated to reproduce the advantageous domain wall properties seen in nanotubes. Using a dipolar-coupled domain wall pair in a trilayer, we show that nanotubular dynamics are accessible within structures that can be made using standard lithographic methods.

2. Micromagnetic Model

Magnetization dynamics of domain walls in trilayer structures were investigated using the finite difference micromagnetic software OOMMF to solve the Landau-Lifshitz-Gilbert equation.[32] The 100 nm wide trilayer consisted of two 2 nm thick Permalloy (Py, $Ni_{80}Fe_{20}$) layers either side of a 1 thick nm non-magnetic spacer [Fig. 1(a)]. Transverse domain walls were initialized at similar locations in both the top and bottom layers and propagated along a 2.7 μm long section of wire using a constant magnetic field. For comparison, domain walls were also modelled in Permalloy wires corresponding to an isolated single layer from the trilayer structure (100 nm wide, 2 nm thick). All models used $5×5×1$ nm^3 cells and standard material constants for Permalloy: saturation magnetization $M_s = 8×10^5$ A/m, exchange stiffness $A = 1.3×10^{-11}$ J/m, magneto-crystalline anisotropy constant $K = 0$ J/m^3 and damping factor $α = 0.02$. Modelling the spacer layer as an insulator to inhibit RKKY interactions, interlayer exchange coupling was neglected. To prevent the domain walls being driven out of the wire by demagnetization fields during initialization and to minimize end effects, the magnetization up to 300 nm from each end of the wire was frozen along the wire axis.

3. Results of the Numerical Experiment and Discussion

Dipolar interactions between the transverse domain walls in the top and bottom layers meant that they formed a composite domain wall structure when magnetized anti-parallel [Fig. 1(b)]. Trilayer with parallel domain wall magnetizations were energetically unfavorable, with walls initialized parallel to each other quickly separating due to repulsion between the magnetic charges on both the wall magnetization and domain magnetization. Notably, the anti-parallel domain wall configuration is reminiscent of the domain wall structure found in tubular nanowires [Fig. 1(c)], creating a circulating magnetic induction pattern around the composite domain wall due to the combination of the individual wall magnetizations and resultant stray fields [Fig. 1(a), dashed line].

Two configurations of composite domain wall were investigated, which we treat as separate chiral structures. Clockwise (CW) chirality, defined in figures 1(a) and 1(b), has a down-transverse wall in the top layer and an up-transverse wall in the bottom layer, creating a clockwise circulation around the field direction. Correspondingly, anti-clockwise (ACW) chirality is defined by an up-transverse wall in the top layer and a down-transverse wall in the bottom layer. Figure 2(a) shows that the quasi-tubular composite structure affected the dynamic behavior of the constituent domain walls. Similar to behavior in thicker wires,[16] isolated layers of 2 nm thick Py exhibited three distinct regimes of domain wall motion, characterized by

steady-state propagation [Fig. 2(a), squares, H < 40 Oe], periodic Walker breakdown [Fig. 2(a), squares, 40 Oe < H < 70 Oe] and spin-wave suppression of Walker breakdown [Fig. 2(a), squares, H > 70 Oe]. During steady-state propagation, wall velocity increased monotonically with applied field, but above the Walker breakdown field (H_W = 40 Oe) further increases in field reduced the average wall velocity due to the periodic retrograde motion following reversal of wall magnetization via anti-vortex nucleation. Domain wall velocities for both chirality states in the trilayer were faster than in isolated layers, even below the Walker breakdown field of the isolated layer, but the most striking feature of the composite domain wall dynamics is the absence of Walker breakdown [Fig, 2(a), circles and triangles]. Composite walls did not experience the periodic retrograde motion associated with Walker breakdown, even at fields much higher than the Walker breakdown field seen in the isolated single layer [Fig. 2(b)]. Nevertheless, the Walker breakdown field of the isolated layer did mark a change in composite wall dynamics, with the composite wall mobility decreasing considerable around H_x = 40 Oe. This behavior is analogous to wall motion in tubular wires,[28] where a distinct decrease in the domain wall mobility at a critical field is caused by a Cherenkov-like spin wave emission. Also mimicking tubular systems[30,29], the composite wall dynamics broke chiral symmetry, with CW-walls generally travelling faster than ACW walls [Fig. 2(a)]. However, the analogy with tubular dynamics is not exact, as both chiralities in the trilayer were able to completely suppress the retrograde motion associated with Walker breakdown [Fig. 2(b)].

Motion in fields above the Walker breakdown field of its constituent layers had remarkably little effect on the stability of the composite domain wall structure. Figure 3 shows that the individual domain walls in the top and bottom layers of the CW-wall retained their relative positions when propagated by a 60 Oe field, with the wall in the top layer being positioned directly above the wall in the bottom layer throughout motion. Similar behavior was seen in the ACW-walls. Given that exchange interactions were neglected from these models, the stability must be due to the stray field contributions from the domain wall magnetizations. Transverse stray field components from one wall were directed in alignment with the magnetization of the other, reinforcing the magnetization configuration of the composite structure. Unlike when global transverse fields are applied,[26] the localized nature of the stray fields means they increased the domain wall width without canting the domains either side of the wall, but would still counteract Walker breakdown. Another contribution to the Walker breakdown suppression could feasibly be the out-of-plane component of the stray field interactions between the domain walls, via the core polarity reversal mechanism identified by Kunz and Reiff.[24]

To identify which mechanism was responsible for Walker breakdown suppression, Figure 4 examines the magnetization structure of the composite domain wall with CW chirality in the trilayer during wall motion under various fields that would produce steady-state propagation (20-40 Oe), periodic Walker breakdown (60 Oe) or spin-wave suppressed Walker breakdown (100 Oe) in the individual constituent layers. Similar behavior was also observed in ACW-walls. At the lowest field [Fig. 4(a)], the domain walls in each layer propagated with a transverse structure that was slightly distorted by the stray field from the adjacent layer, but largely similar to that found in isolated layers, as may be expected within the steady-state propagation regime. The transverse structure and chirality were maintained as the field was increased [Figs. 4(b) and 4(c)], even above the Walker breakdown field of the constituent layers [Figs. 4(d) and (e)]. While the preservation of the composite structure was analogous to the behavior of domain walls in nanotubes, details of the structure were unique to the planar system. Wall motion was accompanied by an in-plane canting of the wall structure, which occurred in opposite directions in the top and bottom layers due to their opposite wall magnetizations. Together with effects of the stray field from each layer, this redistributed the magnetic charges around each wall, effectively increasing the wall width. This may have contributed to the increase in composite wall speed compared with transverse walls in single layers [Fig. 2(a)]. Above 100 Oe, the walls in each layer periodically nucleated anti-vortices [highlighted in Figs. 4(f) and (g)], indicating that the underlying Walker breakdown mechanism was still present. However, the anti-vortices were quickly shed, so the Walker breakdown was suppressed and wall chirality was preserved throughout motion (movie available in the Supplementary Material SM1). This behavior is identical to that seen under uniform transverse fields,[26] demonstrating the influence of the transverse stray field from the domain wall in the other layer. As the anti-vortex core polarization did not switch during the shedding [Fig. 4(g)], the out-of-plane components of the stray field cannot be responsible for the Walker breakdown suppression. Therefore, Walker breakdown suppression in this structure can only be due to the transverse stray field interactions between the domain walls in each layer.

In addition to displaying the domain wall structure, Figs. 4(b)-(e) also indicate that wall propagation was associated with spin wave emission above a critical drive field. This emission was reminiscent of the Cherenkov-like spin wave emission seen in transverse walls in tubular nanowires.[28,31] Dynamically, the onset of spin wave emission at 30 Oe coincided with an abrupt drop in domain wall mobility [Fig. 2(a)], from around 27 m/s/Oe between 10 Oe to 30 Oe to less than-0.3 m/s/Oe above 30 Oe. As has been observed in tubular wires,[28] the decrease in wall mobility was due to the increase in energy dissipated by the spin waves, which increases the effective domain wall mass in the wall's equation of motion. In the trilayer system, increases in spin wave amplitude (domain wall mass) quickly counteracted the larger drive forces at higher

fields, so unlike the tubular system the trilayer was limited to a maximum velocity.

Characteristics of the spin waves are shown in more detail in Fig. 5 for a composite CW-domain wall moving under axial fields. Although there were no spin waves present at 20 Oe, spin waves were emitted at 30 Oe. This was below the Walker breakdown field of the constituent layers and was not seen in the single layer model, indicating that the emission occurs through a mechanism independent of Walker breakdown caused by the arrangement of the composite domain wall. Spin wave emission was non-reciprocal, with spin waves emitted ahead of the domain wall having a shorter wavelength and shorter decay length than spin waves emitted behind the domain wall. Additionally, the emitted spin waves travelled at the same speed as the domain wall (Fig. 3). All of these characteristics are consistent with the mechanism of Cherenkov-like spin wave generation seen in tubular wires.[28] Since spin waves display a minimum phase velocity in their dispersion curve, walls moving below the minimum phase velocity do not emit any spin waves. When domain walls are travelling faster than the minimum spin wave phase velocity, energy from the moving wall is dissipated by two wavevectors (corresponding to short and long wavelengths), propagating in either direction from the wall with phase velocities matching the wall velocity. Interestingly, similar Cherenkov-like spin wave generation also occurs when a localized field source is propagated faster than the minimum spin wave phase velocity.[33] This indicates that there were two potential sources of spin wave excitation in the trilayer: firstly, the fast motion of each domain wall in their respective layers and secondly, the moving stray field from their partner wall in the other layer.

In a departure from the analogy with nanotubes, ACW-domain wall exhibited similar dynamic behavior to the CW-walls, except that the domain walls had lower velocities and slightly narrower wall widths. Walker breakdown suppression was mediated via a similar mechanism of vortex shedding to CW-walls (movie available in Supplementary Material SM2). Spin waves were emitted under similar field conditions to CW-walls, with emission triggered as the domain wall velocity plateaued above 30 Oe, but not at lower fields. This was unexpected, as Fig. 2(a) shows that the wall velocities achieved during the velocity plateau in the ACW-wall were slower than the CW-walls under a 20 Oe field, which did not produce Cherenkov-like spin waves [Fig. 5(a)].

A side-by-side comparison of the spin waves emitted by the CW- and ACW-walls under identical field conditions (60 Oe, Supplementary Materials SM3) shows that there were differences in the spin wave characteristics. The forward propagating spin waves from the CW- and ACW-walls were similar in wavelength, but the ACW-wall emissions had smaller amplitude. On the other hand, the backwards propagating spin waves from the CW- and ACW-

walls had substantially different wavelengths. Additionally, as Cherenkov-like spin waves travel at the same velocity as the domain wall generating them, the spin waves from the ACW-wall were slower than minimum phase velocity of spin waves emitted from the CW-wall. Taken together, these differences indicate that not only are the domain wall dynamics modified by the composite wall chirality, but the spin wave dispersion curve also has a chiral dependency due to the stray field interactions between propagating spin waves.

4. Conclusion

In conclusion, the dynamics of dipolar-interacting transverse domain walls in a trilayer were found to be distinct from the behavior of domain walls in single-layered wires. Velocity of domain walls in the trilayer coupled with the most favorable chirality was enhanced to more than 32% of the maximum velocity in isolated constituent layers before the Walker breakdown occurs. Stray field interactions between the domain walls in the individual layers meant they behaved as if they were a composite domain wall with properties similar to those found in tubular structures. Only antiparallel wall configurations were stable, so the structure of the composite wall mimicked the circulating magnetization found in tubular wires. The composite wall retained its structure when moving under an applied field and, like a tubular domain wall, moved with a chirality-dependent velocity. Neither of the composite chiralities experienced Walker breakdown. Instead, beyond a critical field, high-speed domain wall motion induced local Cherenkov-type spin wave emission, leading to a dramatic decrease in the mobility of the walls. Emitted spin waves propagated in both forward and backward directions away from the domain wall, but with direction-dependent wavelength and decay length. Taken together, this means that the dipolar-coupled trilayer system produces quasi-tubular domain walls, reproducing the advantageous magnetization dynamics of the tubular system while retaining the planar geometry compatible with standard lithography techniques.

Supplementary Material

See supplementary material for videos of domain wall motion in the trilayer at 100 Oe, showing the mechanism of Walker breakdown suppression for CW-walls (Supplementary Material SM1) and ACW-walls (Supplementary Material SM2) and for a comparison of spin wave emission at 60 Oe from CW- and ACW-walls (Supplementary Material SM3).

Data Availability Statement

The data that support the findings of this study are openly available in Figshare

(https://royalholloway.figshare.com/) at http://358 doi.org/10.17637/rh.16783276.

References

[1] S.S.P.P. Parkin, M. Hayashi, and L. Thomas, Science **320**, 190 (2008).

[2] D.A. Allwood, G. Xiong, C.C. Faulkner, D. Atkinson, D. Petit, and R.P. Cowburn, Science **309**, 1688 (2005).

[3] B. Borie, A. Kehlberger, J. Wahrhusen, H. Grimm, and M. Kläui, Phys. Rev. Appl. **8**, 024017 (2017).

[4] V.D. Nguyen, O. Fruchart, S. Pizzini, J. Vogel, J.-C. Toussaint, and N. Rougemaille, Sci. Rep. **5**, 12417 (2015).

[5] Y. Nakatani, A. Thiaville, and J. Miltat, J. Magn. Magn. Mater. **290–291**, 750 (2005).

[6] V. Estévez and L. Laurson, Phys. Rev. B **91**, 054407 (2015).

[7] D. Atkinson, D.A. Allwood, G. Xiong, M.D. Cooke, C.C. Faulkner, and R.P. Cowburn, Nat. Mater. **2**, 85 (2003).

[8] T. Ono, H. Miyajima, K. Shigeto, K. Mibu, N. Hosoito, and T. Shinjo, Science **284**, 468 (1999).

[9] S. Emori, U. Bauer, S.-M. Ahn, E. Martinez, and G.S.D. Beach, Nat. Mater. **12**, 611 (2013).

[10] G.S.D. Beach, M. Tsoi, and J.L. Erskine, J. Magn. Magn. Mater. **320**, 1272 (2008).

[11] J. Han, P. Zhang, J.T. Hou, S.A. Siddiqui, and L. Liu, Science **366**, 1121 (2019).

[12] S.-H. Oh, S.K. Kim, J. Xiao, and K.-J. Lee, Phys. Rev. B **100**, 174403 (2019).

[13] J. Dean, M.T. Bryan, T. Schrefl, and D.A. Allwood, J. Appl. Phys. **109**, 1 (2011).

[14] M.T. Bryan, J. Dean, and D.A. Allwood, Phys. Rev. B **85**, 144411 (2012).

[15] N.L. Schryer and L.R. Walker, J. Appl. Phys. **45**, 5406 (1974).

[16] J.-Y. Lee, K.-S. Lee, S. Choi, K.Y. Guslienko, and S.-K. Kim, Phys. Rev. B **76**, 184408 (2007).

[17] M. Hayashi, L. Thomas, C. Rettner, R. Moriya, and S.S.P.P. Parkin, Nat. Phys. **3**, 21 (2007).

[18] G.S.D. Beach, C. Nistor, C. Knutson, M. Tsoi, and J.L. Erskine, Nat. Mater. **4**, 741 (2005).

[19] L. O'Brien, D. Petit, H.T. Zeng, E.R. Lewis, J. Sampaio, A. V. Jausovec, D.E. Read, and R.P. Cowburn, Phys. Rev. Lett. **103**, 077206 (2009).

[20] T.J. Hayward, M.T. Bryan, P.W. Fry, P.M. Fundi, M.R.J. Gibbs, M.-Y. Im, P. Fischer, and D.A. Allwood,

Appl. Phys. Lett. **96**, 052502 (2010).

[21] S. Krishnia, I. Purnama, and W.S. Lew, Appl. Phys. Lett. **105**, 042404 (2014).

[22] A. Hrabec, V. Křižáková, S. Pizzini, J. Sampaio, A. Thiaville, S. Rohart, and J. Vogel, Phys. Rev. Lett. **120**, 227204 (2018).

[23] K.A. Omari and T.J. Hayward, Sci. Rep. **7**, 17862 (2017).

[24] A. Kunz and S.C. Reiff, Appl. Phys. Lett. **93**, 082503 (2008).

[25] S. Glathe, R. Mattheis, and D. V. Berkov, Appl. Phys. Lett. **93**, 072508 (2008).

[26] M.T. Bryan, T. Schrefl, D. Atkinson, and D.A. Allwood, J. Appl. Phys. **103**, 073906 (2008).

[27] D.M. Burn and D. Atkinson, Appl. Phys. Lett. **102**, 242414 (2013).

[28] M. Yan, C. Andreas, A. Kákay, F. García-Sánchez, and R. Hertel, Appl. Phys. Lett. **99**, 122505 (2011).

[29] J.A. Otálora, J.A. López-López, P. Vargas, and P. Landeros, Appl. Phys. Lett. **100**, 72407 (2012).

[30] M. Yan, C. Andreas, A. Kákay, F. García-Sánchez, and R. Hertel, Appl. Phys. Lett. **100**, 252401 (2012).

[31] R. Hertel, J. Phys. Condens. Matter **28**, 483002 (2016).

[32] M. Donahue and D. Porter, OOMMF User's Guid. Version 1.0, Interag. Rep. NISTIR 6376, NIST, Gaithersburg, MD (1999).

[33] M. Yan, A. Kákay, C. Andreas, and R. Hertel, Phys. Rev. B **88**, 220412 (2013).
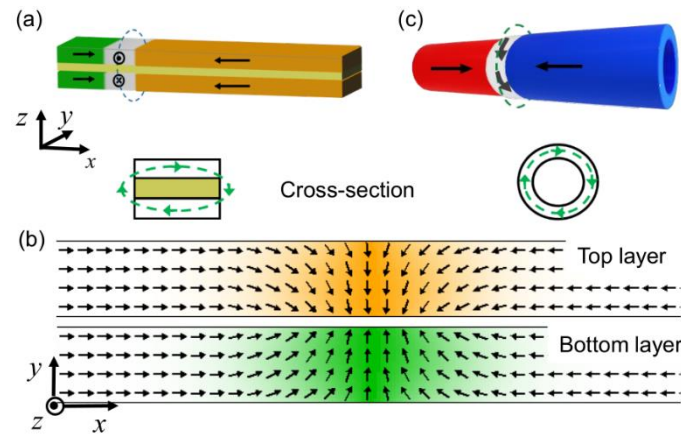
Figures

Fig. 1. (a) Schematic diagram of a composite domain wall in a planar trilayer, with the cross-section highlighting the circulation of magnetic induction (dashed lines) due to the wall magnetization at the center of the wall. Composite domain walls are defined with clockwise (CW) chirality. (b) Micromagnetic calculations of the stable composite (CW) domain wall structure, showing the individual transverse domain walls in the top and bottom Py layers under zero field. Anti-clockwise (ACW) walls are defined with the opposite wall magnetization in each layer. (c) Schematic diagram of a tubular nanowire containing a transverse domain wall, with cross-section indicating the magnetic induction (dashed lines) within the center of the wall.
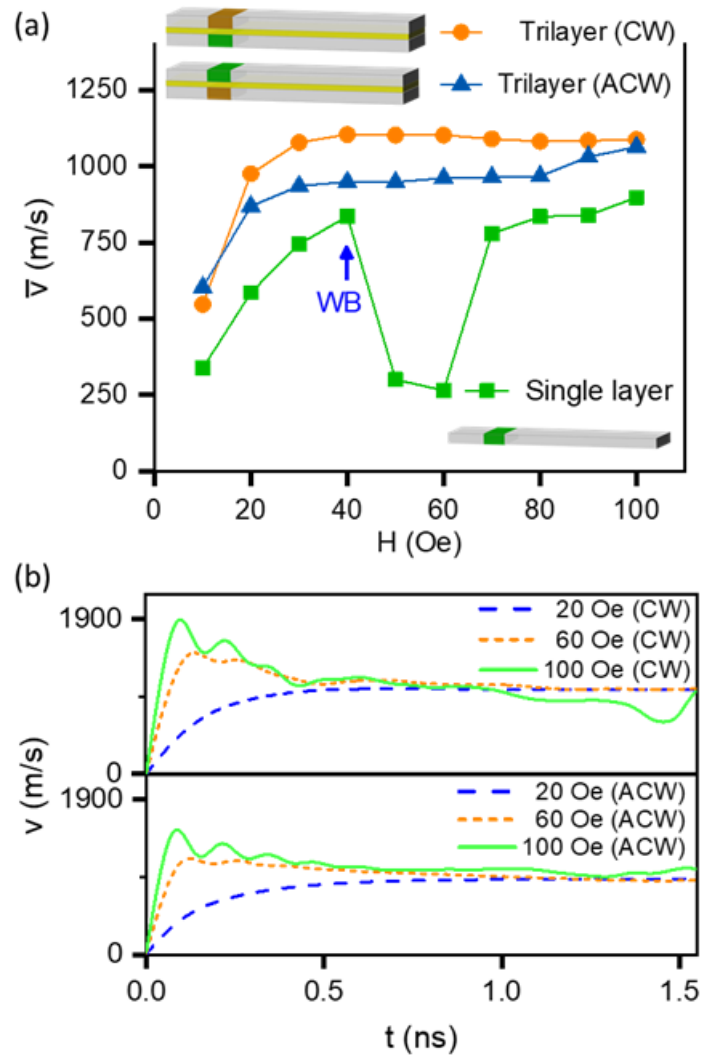
Fig. 2. (a) Field (H) dependence of the average domain wall velocity ($\bar{v}$) in an isolated 2 nm thick Py single layer and in the trilayer structure for both chirality states. The blue arrow marks the Walker breakdown field (WB) of the isolated Py single layer. (b) Instantaneous domain wall velocity v in the trilayer structure with both chirality states under H = 20 Oe (dashed line), 60 Oe (dotted line) and 100 Oe (solid line).
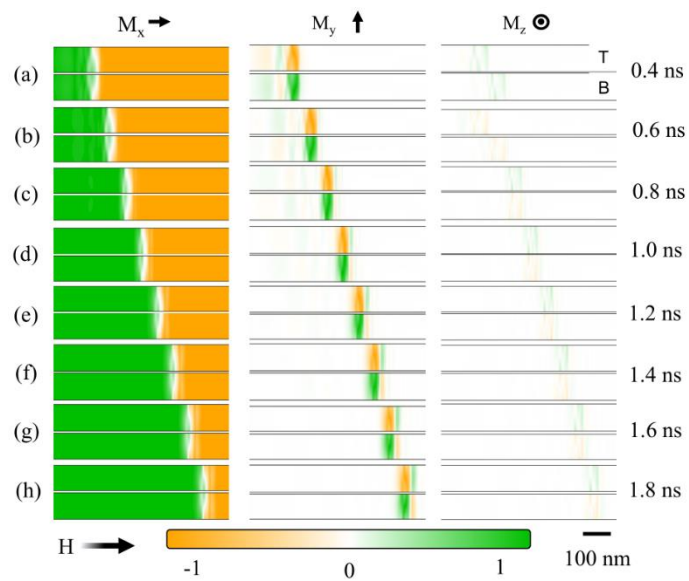
Fig. 3. (a)–(h) show the time evolution of the transverse domain wall magnetization configuration during propagation of a CW-wall along the trilayer wire under H_x = 60 Oe (above the Walker breakdown field of a single Permalloy layer). Upper and lower images represent magnetization in the top layer (T) and the bottom layer (B), respectively.
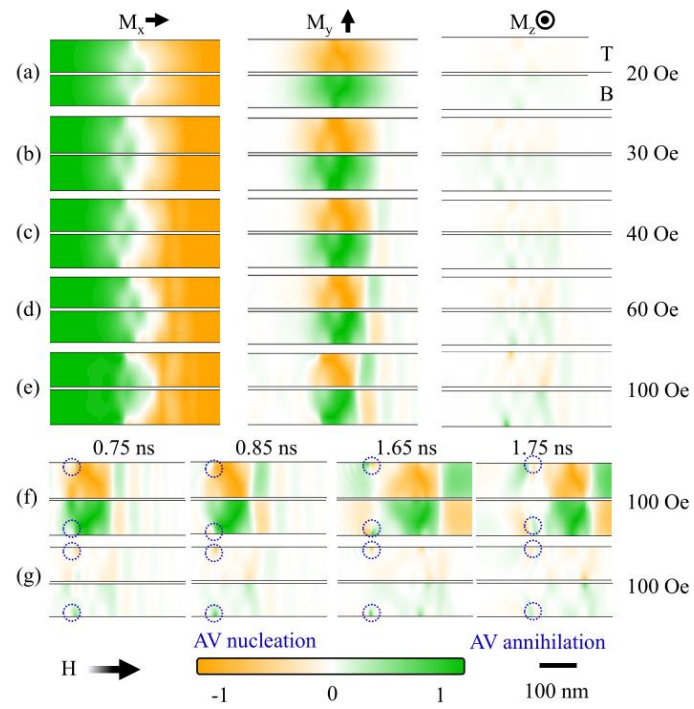
Figure 4: The magnetization configuration of domain walls with CW chirality in the trilayer moving under external fields of H = (a) 20 Oe, (b) 30 Oe, (c) 40 Oe, (d) 60 Oe, (e) 100 Oe. Snapshots of (f) the M_y- and (g) the M_z-component around anti-vortex (AV) nucleation and annihilation for the H = 100 Oe data. For reference, the timepoint shown in (e) is at 0.85 ns. In all cases, upper and lower images represent magnetization in the top layer (T) and the bottom layer (B), respectively.
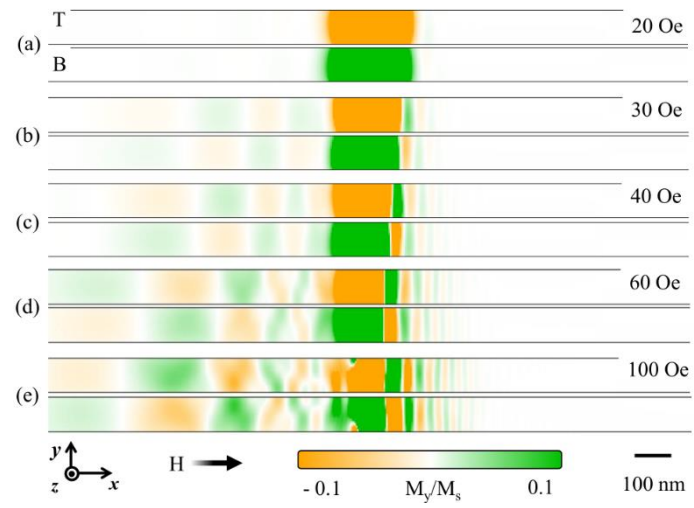
Figure 5. Spin wave emission by a composite domain wall with CW chirality moving under various axial fields, showing the M_y magnetization components of the top (T) and bottom (B) layers of the trilayer (upper and lower images, respectively).